J. Biochem. 125, 270-276 (1999)

Time-Resolved Measurements of Photovoltage Generation by Bacteriorhodopsin and Halorhodopsin Adsorbed on a Thin Polymer Film[1]

Eiro Muneyuki,*,[2] Chie Shibazaki,† Hiroyuki Ohtani,† Daichi Okuno,* Makoto Asaumi,* and Tatsushi Mogi‡

*Research Laboratory of Resources Utilization and †Department of Biomolecular Engineering, Faculty of Bioscience and Biotechnology, Tokyo Institute of Technology, Nagatsuta 4259, Midori-ku, Yokohama 226-8503; ‡Department of Biological Sciences, Graduate School of Science, The University of Tokyo, Hongo, Bunkyo-ku, Tokyo 113-0033

Received September 22, 1998; accepted October 19, 1998

We constructed a time-resolved photovoltage measurement system and examined the photovoltage kinetics of wild-type bacteriorhodopsin, its D96N mutant, and halorhodopsins from *Halobacterium salinarum* and *Natronobacterium pharaonis*. Upon illumination with a laser flash, wild-type bacteriorhodopsin showed photovoltage generation with fast (10-100 μs range) and slow (ms range) components while D96N lacked the latter, as reported previously [Holz, M., Drachev, L.A., Mogi, T., Otto, H., Kaulen, A.D., Heyn, M.P., Skulachev, V.P., and Khorana, H.G. (1989) *Proc. Natl. Acad. Sci. USA* 86, 2167-2171]. In contrast, photovoltage generation in halorhodopsins from *H. salinarum* and *N. pharaonis* was significant only in the ms time range. On the basis of the photovoltage kinetics and photocycle, we conclude that major charge (chloride) movements within halorhodopsin occur during the formation and decay of the N intermediate in the ms range. These observations are discussed in terms of the "Energization-Relaxation Channel Model" [Muneyuki, E., Ikematsu, M., and Yoshida, M. (1996) *J. Phys. Chem.* 100, 19687-19691].

Key words: bacteriorhodopsin, halobacteria, halorhodopsin, photocycle, photovoltage.

Time-resolved electrical measurement of charge movement is a powerful technique for probing the electrogenic transport processes by ion-pumping proteins. Drachev *et al.* (*1, 2*) developed a novel system in which membrane fragments (or vesicles) were adsorbed onto supporting black lipid membranes and demonstrated the electrogenicity of a variety of ion pumps. Subsequently, collodion films (*3*) and porous filters impregnated with a lipid solution (*4*) were introduced as more stable supports.

For bacteriorhodopsin (bR) from *Halobacterium salinarum*, this technique revealed that the fast and the slow components in the photovoltage generation are associated with the formation and the decay of the M intermediate, respectively (*5, 6*). Subsequently, in combination with site-directed mutagenesis, it was shown that Asp96 is crucial for the reprotonation of the Schiff base during M decay and for proton uptake from the cytoplasm (*7-9*). In contrast, Asp85 was suggested to be involved in proton release during M formation (*10, 11*). Recent crystallographic studies (*12, 13*) provided a structural basis for the critical roles of Asp96 and Asp85 in the proton uptake and release channels, respectively.

Halorhodopsin (hR), an alternative light-driven ion pump, is present in the cytoplasmic membranes of *Halobacterium salinarum* (*H. salinarum*) and *Natronobacterium pharaonis* (*N. pharaonis*). It translocates chloride ions in the opposite direction to the H^+ pumping by bR (*14, 15*). Spectroscopic studies indicated that the photocycle of hR can be described as "$HR \xrightarrow{h\nu} K \rightarrow L \leftrightarrow N(\leftrightarrow O) \rightarrow HR$" (*14, 15*), although controversies remain. In contrast to bR, previous electrical studies are not yet sufficient to identify the chloride transport step(s) in the hR photocycle (*16-19*). For example, the photovoltage changes in hR from *N. pharaonis* (phR), which were reported quite recently by Kalaidzidis *et al.* (*19*), are consistent with the photocycle of hR from *H. salinarum* (shR) (*20*) rather than that of phR reported by Váró *et al.* (*21, 22*). Thus, the ion translocation step(s) in the hR photocycle remains to be studied.

Previously, we developed a method to adsorb membrane fragments onto a stable thin polymer film, that enables us to examine the photoelectric response by bR (*23*). In the present study, we carried out time-resolved measurements of photovoltage changes of bR and hR in the μs-s time range. We also carried out time-resolved measurements of spectroscopic change due to the photocycle of hR and conclude that chloride translocation by hR occurs during the formation and decay of the N intermediate. These observations are further discussed in terms of the "Energization-Relaxation Channel Model" (*24*).

[1] This work was supported in part by Grants-in-Aid for Scientific Research on Priority Areas (09257217 to EM, 08249106 and 09257213 to TM), and for Scientific Research (C) (09833001 to EM) and (B) (08878097 to TM) from the Ministry of Education, Science, Sports and Culture of Japan.

[2] To whom correspondence should be addressed. Phone: 045-924-5232, Fax: 045-924-5277, E-mail: emuneyuk@res.titech.ac.jp

Abbreviations: bR, bacteriorhodopsin; D96N, a mutant bR where Asp96 is replaced by Asn; hR, halorhodopsin; shR, hR from *Halobacterium salinarum*; phR, hR from *Natronobacterium pharaonis*.

MATERIALS AND METHODS

Materials—A recombinant *H. salinarum* strain that over-expresses the D96N mutant of bR was a kind gift from Dr. J.K. Lanyi (University of California, Irvine). The over-producing strains of shR and phR were kind gifts from Dr. R. Needleman (Wayne State University). Membrane fragments containing bR or hR were isolated by sucrose density gradient centrifugation (*25*). Purple membranes containing the wild-type bR and D96N were treated as described previously (*23*). The shR-overproducing membranes were suspended in 20 mM Tris-maleate buffer containing 4 M NaCl and 2 mM $MgCl_2$ (pH 7.0; denoted as buffer A). Typically, the concentration was adjusted to $A_{570}=1.5$ (1 cm light pass). The phR-overproducing membranes were concentrated using Centricon 10 (Amicon; Beverly, MA) and used without sucrose removal.

Setup for Electrical Measurement—The system consists of a chamber connected to a home-made high-input impedance amplifier with light shielded Ag-AgCl electrodes, and a laser flash system triggered by a personal computer (Fig. 1). A 0.9-μm-thick polyester film (Lumirror; Toray, Tokyo), to which membrane fragments were adsorbed, was placed between the two compartments of the chamber. A 0.5 GΩ shunt resister was inserted between the inverting and non-inverting input of the amplifier IC (LF356N) to set the input impedance. The chamber and the amplifier were placed in a shield box that avoids mechanical vibration and electric noise. The Nd-YAG laser (532 nm; Surelite I-10, Continuum, Santa Clara, CA) was triggered by a personal computer equipped with a high-speed AD converter (2 MHz maximum, model EC2372A-1; Elmec, Tokyo). Data were collected every μs and stored in removable media on the personal computer.

Adsorption of Membrane Fragments and Photovoltage Measurement—The adsorption of the shR- and phR-overproducing membranes to the film was carried out as described for purple membranes (*23*). Briefly, 80 μl of membrane suspension was applied directly to one side of the polyester film in the chamber and left for 40 min at room temperature. Excess membranes were removed by pipetting, and 1.5 ml of buffer A was added to both compartments. For measurements of shR, the buffer in the membrane-adsorbed side compartment was exchanged twice with NaCl-free buffer A to wash out residual unbound membranes and chloride ions. Subsequently, after 1-3 min incubation with buffer A containing 0.5% octylglucoside, the chamber was washed several times and filled with buffer A. In the case of phR, the adsorbed membranes were incubated with 50 mM Tris-maleate (pH 7.0) containing 0.1 M $CaCl_2$ and 0.1% octylglucoside for 2 min, and washed with the same buffer without octylglucoside.

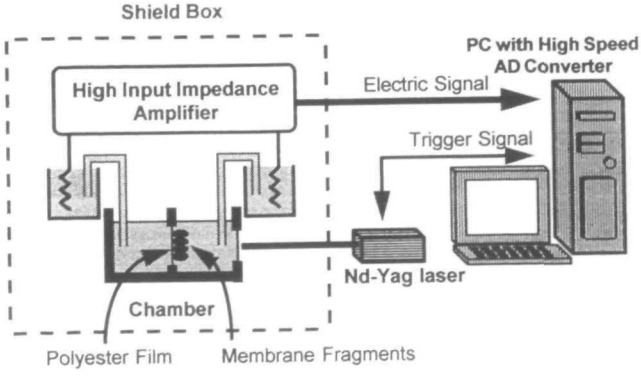

Fig. 1. **A schematic description of the time-resolved photovoltage measurement system.** See "MATERIALS AND METHODS" for details.

Photovoltage measurements of wild-type bR, D96N, and phR were carried out at room temperature in 25 mM Tris-HCl (pH 7.2) containing 0.1 M NaCl. For shR, the NaCl concentration was raised to 3 M to obtain a larger response. Photoexcitation was carried out at 532 nm with the Nd-YAG laser and the data were stored as described above.

Photochemical Cycle Measurements—The main configuration of the laser flash photolysis apparatus has been described elsewhere (*26*). Membrane suspensions (1 cm light pass) were excited by a second harmonic (532 nm) of a Q-switched Nd-YAG laser (Surelite I-10 or Minilite, Continuum). A continuous wave xenon lamp (150 W, L2274, Hamamatsu Photonics, Shizuoka) was used as a probe light source with a heat-absorption water cell, neutral density filters, and UV cut-off glass filters. The transmitted probe light was detected with a photomultiplier (R3825, Hamamatsu Photonics) coupled to a grating monochromator ($f=100$ mm, 150 grooves/mm, CT10, JASCO, Tokyo). Laser scattering was rejected by appropriate sharp cut-off filters. The output signals from the photomultiplier were stored and averaged with an AD converter (APC-204, Autonics, Kanagawa).

RESULTS AND DISCUSSION

Time-Resolved Photovoltage Measurements of bR and hR—The photovoltage kinetics reflect charge movement (*i.e.*, proton translocation) in the protein during a single turnover of the bR photocycle. As reported previously (*6, 7*), there are fast (10-100 μs range) and slow (ms range) components in wild-type bR (Fig. 2A). A logarithmic plot in the time range from 1 μs to 2 s (Fig. 2B) is similar to that obtained with a planar lipid membrane (*7*). The fast component in the 10-100 μs range corresponds to M formation, when the protonated Schiff base deprotonates and the proton migrates to Asp85 (*10*). The slow component in the ms range corresponds to the M decay that accompanies the proton transfer from Asp96 to the deprotonated Schiff base (*7-9*). A subsequent recovery to the original level (>20 ms) corresponds to the system discharge (*5*). In D96N, the slow component is absent due to the lack of the direct proton donor for the deprotonated Schiff base (*7-9*) (Fig. 2, C and D).

Next, we examined the photovoltage kinetics in shR and phR, and found that in both cases a large photovoltage change took place only in the ms time range (Fig. 3, AB and CD for shR and phR, respectively). The absence of the fast component in the 10-100 μs range characteristic of bR (Fig. 2, A and B) is consistent with the lack of the M-like intermediate in the hR photocycle, *i.e.* the Schiff base remains protonated.

The slow component was analyzed as the sum of the exponents to deduce the time constant(s) of this process. The photovoltage kinetics in shR contain two subcomponents with time constants of about 0.4 and 4 ms. The

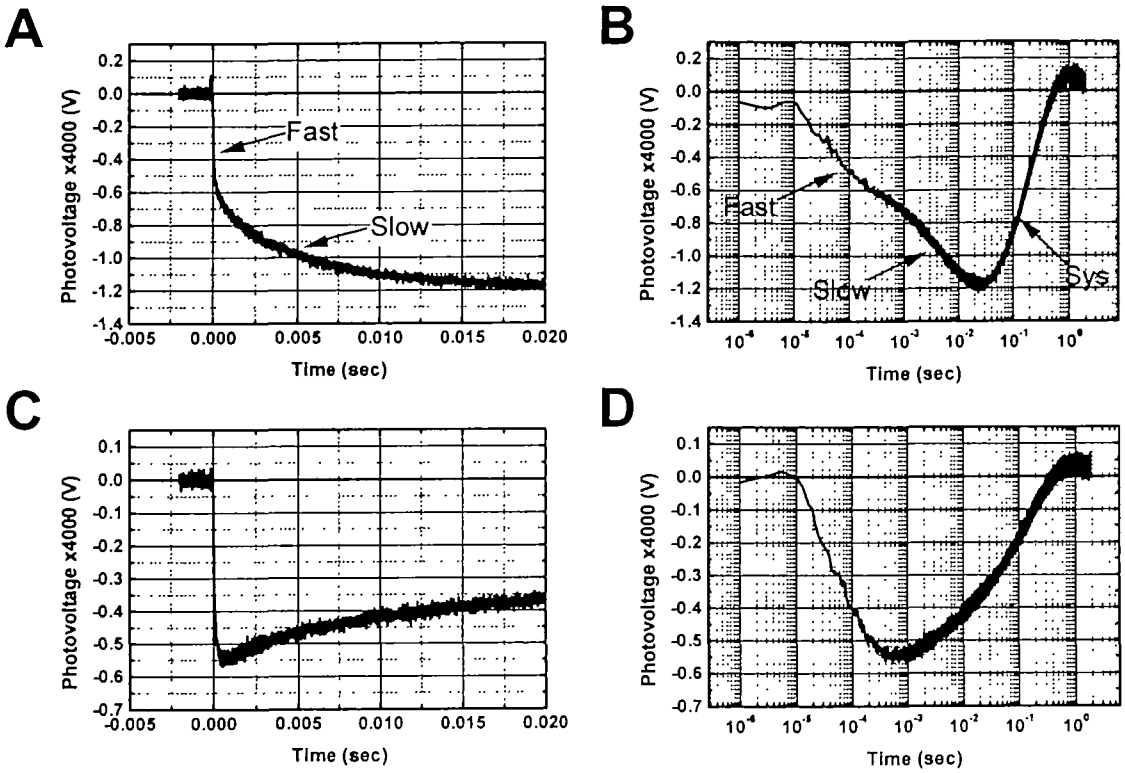

Fig. 2. **Time-resolved photovoltage changes in the wild-type bR (A and B) and D96N (C and D).** A and C show the time-course up to 20 ms on a linear scale. For panels B and D, a logarithmic scale up to 2 s was used. The medium was 25 mM Tris-HCl (pH 7.2) containing 0.1 M NaCl. Measurements were repeated at 1-min intervals, and the accumulation was 9 and 27 for wild-type bR and D96N, respectively. Arrows labeled as "Fast" and "Slow" indicate fast (10-100 μs) and slow (ms) components of the photovoltage change, respectively. The arrow designated "Sys" indicates the system discharge.

ratio of their amplitudes is about 6 : 1. In the case of phR, similar analysis gave two subcomponents with time constants of 0.9 and 2 ms and an amplitude ratio of about 1 : 3.

Time-Resolved Measurement of the hR Photocycle— Visible and infrared spectroscopic studies on shR identified photointermediates more or less equivalent to K (or KL), L, and O of the bR photocycle (*14, 15*). Váró *et al.* (*20*) proposed the all-*trans* photocycle, which is coupled to chloride translocation, as follows:

$$HR \xrightarrow{h\nu} K \longrightarrow L1 \longleftrightarrow L2 \longleftrightarrow N \longrightarrow HR.$$

The L state of shR consists of two substates, L1 and L2 (*20*) [or HR520I and HR520II (*27*)], that may play a critical role in chloride pumping, as shown for the two M substates in proton pumping by bR (*28*). However, this model does not contain any chloride-dependent step. Recently, Rüdiger and Oesterhelt (*27*) pointed out that experimental conditions can alter the sequence of anion uptake and release, which in turn affects the spectroscopic detection of the O-like intermediate in the hR photocycle. On the basis of site-directed mutagenesis studies, they proposed that a chloride ion near Arg108 and Thr111 moves towards the protonated Schiff base during L1 formation. At the spectroscopically silent L1-L2 transition, the accessibility of the protonated Schiff base to chloride ions in the release and uptake channels may switch. Chloride transfer from the protonated Schiff base to the cytoplasm occurs during the decay of the L intermediate (and hence N formation) (*27*). Resonance Raman and Fourier-transform infrared studies have indicated that a bound anion in the vicinity of the protonated Schiff base in HR is transferred to another location in the L state (*29, 30*). Ames *et al.* (*29*) included the O intermediate in the shR photocycle and suggested that the release and uptake of a chloride ion occur during the L-to-O and the O-to-HR transition, respectively.

On the other hand, Váró *et al.* (*21, 22*) proposed the following photocycle scheme for phR:

$$HR \xrightarrow{h\nu} K \longrightarrow L \longleftrightarrow N \longleftrightarrow O \longrightarrow HR' \longrightarrow HR.$$

On the basis of the chloride concentration dependency of the rate constants, they concluded that the N-to-O transition is associated with chloride release and the O-to-HR′ transition with chloride uptake (*22*). The release of a bound chloride ion near the Schiff base (*30-33*) to the cytoplasmic side may be triggered by structural changes in the protein associated with a transient volume decrease in the L-to-N transition and the reisomerization of the retinal (13 *cis* → all *trans*) during the N-to-O transition (*22*).

Quite recently, Kalaidzidis *et al.* (*19*) reported the photovoltage kinetics of phR. A short lag phase observed in their case was attributed to an electrically silent process rather than to a fast (τ = 100-200 μs) electrogenic process followed by an electrically silent process with τ = 1-2 ms (*19*). Based on the results, they concluded that the photovoltage kinetics of phR are consistent with the photocycle model for shR proposed by Váró *et al.* (*20*) rather than that of phR (*21, 22*).

In order to identify the chloride translocation step(s), we

measured the photocycle (Figs. 4 and 5) and photovoltage kinetics (Fig. 3) of shR and phR at the same solute compositions. Upon excitation with the laser flash, shR exhibited an immediate absorbance increase at 504 nm and decrease at 600 nm, indicating rapid L formation (*i.e.*, within 10 μs) (Fig. 4). During N formation, the amount of L intermediate remains relatively constant due to an equilibrium of the photointermediates, and only the K decrease is spectroscopically significant (*20*). The subsequent absorbance increase at 504 nm and slight decrease at 600 nm ($\tau = 0.22 \pm 0.04$ ms) correspond to N formation. The 504-nm decay and 600-nm rise were analyzed as the sum of two exponents ($\tau = 7.6 \pm 0.7$ and 26 ± 2 ms at 504 and 600 nm). The fast and slow phases seem to correspond to the recoveries of all-*trans* HR and 13-*cis* HR, respectively (*20*). We did not find any significant absorbance change at 408 nm because of the absence of an M-like intermediate (data not shown). The absorbance change at 648 nm was attributable to contributions from the HR, K, and N, and does not necessarily require the red-shifted O-like intermediate. Thus, the data obtained here (Fig. 4) are qualitatively consistent with the photocycle scheme reported by Váró *et al.* (*20*). Differences in the time constants between our study and that of Váró *et al.* (*20*) may originate from

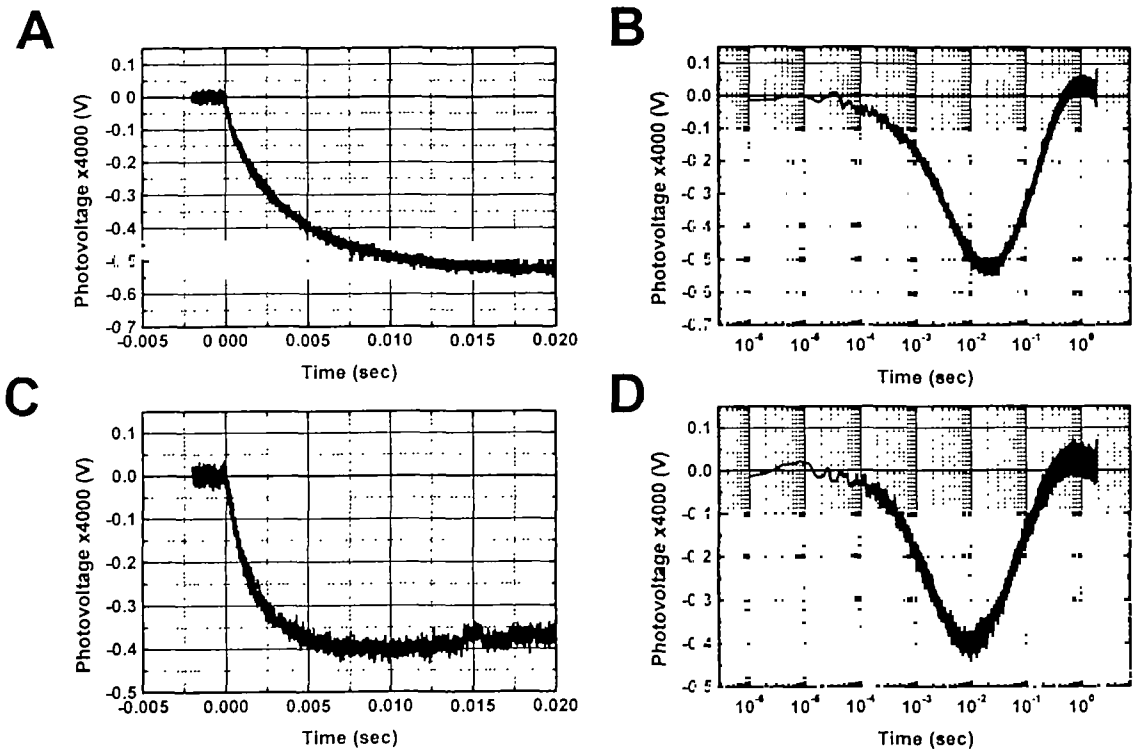

Fig. 3. **Time-resolved photovoltage changes in shR (A and B) and phR (C and D).** Accumulation was 35 and 27 for shR- and phR-overproducing membranes, respectively. The NaCl concentration of the medium for shR was increased to 3 M. Other details are the same as the legend to Fig. 2.

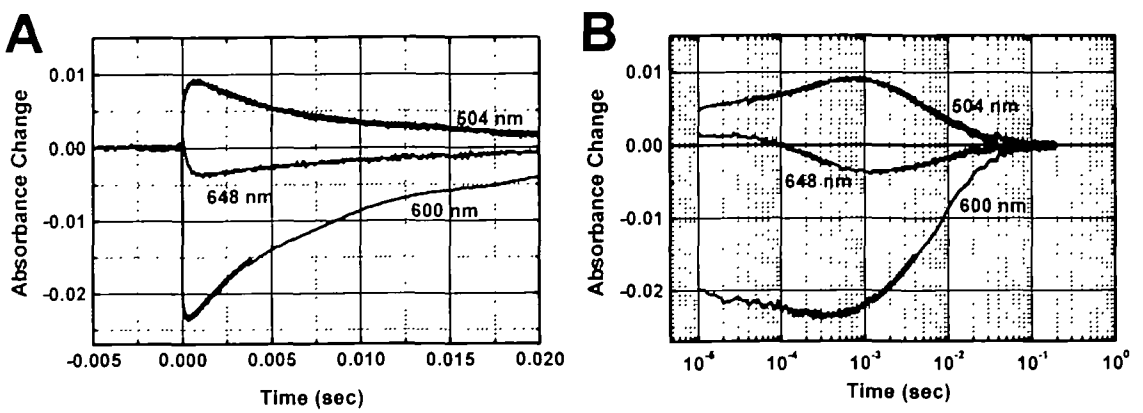

Fig. 4. **Transient absorption changes in shR.** Absorbance changes in shR at the indicated wavelengths are shown up to 20 ms on a linear scale in A and on a logarithmic scale in B. The medium was 25 mM Tris-HCl (pH 7.2) containing 3 M NaCl.

the different temperature and solvent conditions.

In the present study, the phR photocycle (Fig. 5) was somewhat slower than that reported by Váró *et al.* (*21*) and the shR photocycle (Fig. 4). The lifetime of L was estimated to be 2.9±0.4 ms from the decay in the absorbance at 504 nm. Then, the O formation occurs with a time constant of 4.4±1.0 ms, as determined from the build-up of the absorbances at 600, 616, and 640 nm. As reported by Váró *et al.* (*21*), L decay (*i.e.*, N formation) and the O formation occur very closely in time, suggesting a rapid pseudo-equilibrium between the N and O intermediates. Finally, HR recovery concludes the phR photocycle with a time constant of 85±15 ms, as estimated from the temporal slight absorbance increase at 504 nm and decreases at 616 and 640 nm.

Correlation between the Photocycle and Photovoltage Kinetics—Váró *et al.* reported that the L intermediates of shR (*20*) and phR (*21*) form in the μs range and persist until 1 ms after the photoexcitation. Our transient absorption analyses are consistent with their photocycle scheme. The present photovoltage measurements show that the charge movement in the μs time range is insignificant in both shR and phR (Fig. 3). Therefore, chloride translocation during or before L formation, if it occurs, should involve only a short distance or take place through a high dielectric environment. Alternatively, a counter charge may move in the opposite direction.

More importantly, it should be emphasized that the charge transfer in hR occurs mainly in the sub-ms and ms time ranges. In the same time range, optical changes were found also in the time-resolved spectroscopic measurements. From the photovoltage kinetics (Fig. 3) and transient absorption changes (Figs. 4 and 5), we conclude that the chloride translocations with time constants of 0.4 and 4 ms in shR and 0.9 and 2 ms in phR correspond to the formation and decay of the N intermediate (0.22±0.04 and 7.6±0.7 ms, respectively, in shR and 2.9±0.4 and 4.4±1.0 ms, respectively, in phR from the photocycle data), respectively. Small variations in the rate constants between the photovoltage kinetics and transient absorption changes are attributable to differences in the experimental conditions.

Our data on the photovoltage kinetics and photocycles of shR and phR are summarized in Fig. 6. In addition to the photocycle scheme proposed by Váró *et al.* (*20*), we include the O intermediate in the photocycle of shR and put chloride release and uptake before and after the O intermediate according to Ames *et al.* (*28*). On the basis of photovoltage kinetics (this study), the intramolecular chloride translocation (*i.e.*, electrogenic) steps were assigned to the formation and decay of the N intermediate and their time constants and relative amplitudes are indicated. The photocycle of phR was adopted from Váró *et al.* (*21, 22*) and modified by adding electrogenic steps based on the data obtained in this study. It is notable that very similar sequences were deduced for shR and phR with regard to the order of chloride release, uptake, and electrogenic steps.

Energization-Relaxation Channel Model for Chloride

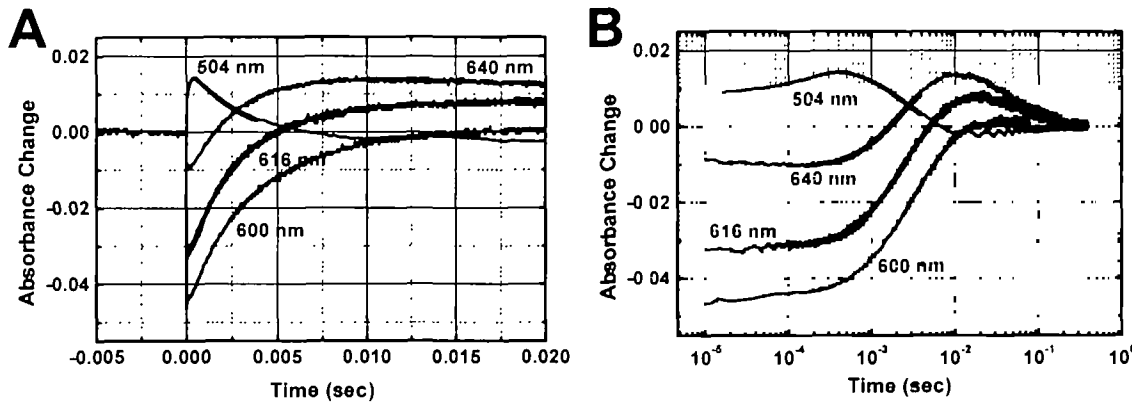

Fig. 5. **Transient absorption changes in phR.** Absorbance changes in phR at the indicated wavelengths are shown up to 20 ms on a linear scale in A and on a logarithmic scale in B. The medium was 25 mM Tris-HCl (pH 7.2) containing 0.1 M NaCl.

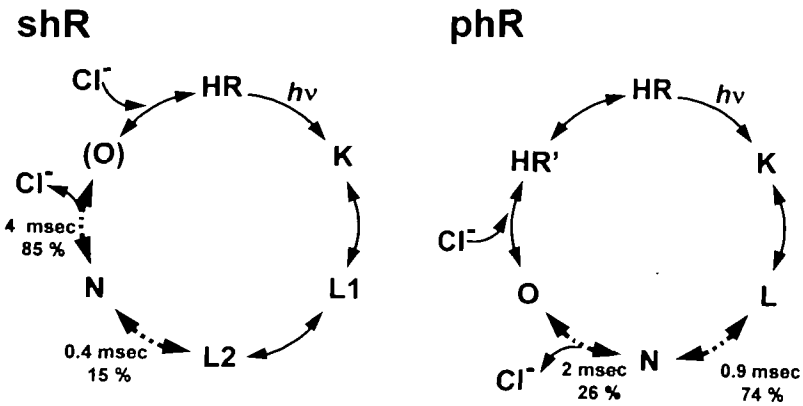

Fig. 6. **Photocycle models for shR and phR showing chloride translocation steps.** The intramolecular chloride translocation (*i.e.*, electrogenic) steps are indicated by broken lines with their rate constants and relative amplitudes. See text for details.

Pumping by hR—The sequence of the release and uptake of chloride ions at the protein surfaces and intramolecular charge movements in hR as described above are in good accordance with our "Energization-Relaxation Channel Model" for proton pumping by bR where unidirectional intramolecular ion transport can be induced by a non-equilibrium transition of the asymmetric potential profile at three ion binding sites (*24*).

Chloride translocation by phR can also be explained by this model which assumes three ion binding sites, A, B, and C (Fig. 7). In the de-energized state, sites A and B are high-affinity binding sites while site C has a low affinity for transported ions. The binding affinities (apparent K_D) of sites A, B, and C for chloride ions in the de-energized state may be estimated as 10, 1, and 150 mM, respectively, based on the K_m value for chloride transport, the spectroscopic titration of chloride binding, and the chloride dependence of the kinetic equilibrium between the N and O intermediates (*21, 22*). Site B could be a chloride binding site in the vicinity of the protonated Schiff base. In the unphotolyzed, de-energized state, chloride ions are bound only to sites A and B. Photo-energization induces a decrease in the binding affinity of site B, which corresponds to the change in the protein-chromophore-chloride interactions in the K-to-L transition. During the L-to-N transition, the bound chloride at site B moves to site C ($\tau = 0.9$ ms). Before the slow relaxation to the high-affinity state of site B by protein conformational change, the release of a chloride ion from site C to the cytoplasmic side occurs due to its low binding affinity during the N-to-O transition (*22*). This step is closely followed by the recovery of the high-affinity state of site B and the migration of the bound chloride ion from site A to site B takes place in an electrogenic manner ($\tau =$ 2 ms). Finally, site A takes up a chloride ion from the extracellular side during the O-to-HR transition (*22*). A resonance Raman study on shR (*29*) suggested that the release and uptake of a chloride ion take place during the formation and decay of the O intermediate. Although the critical role of the O intermediate in chloride transport by shR is somewhat controversial (*20, 27, 29*), the sequence of the elementary processes in chloride pumping by phR may also hold for shR. The Energization-Relaxation Channel Model (*24*) is based on the simple principle of unidirectional ion translocation by non-equilibrium transition of asymmetric potential and, with appropriate modifications, may be applicable to a variety of ion pumps.

Finally, we would like to point out that the application of time-resolved electrical measurements will provide new insights into the molecular mechanisms of other ion pumps such as cytochrome *c* oxidase and ATP synthase by using the flow-flash technique and caged-ATP, respectively.

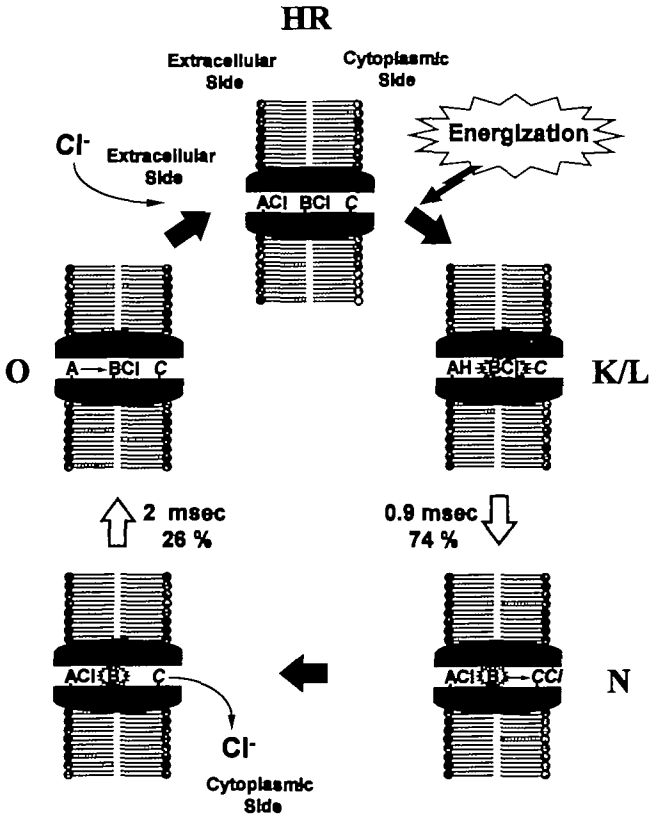

Fig. 7. **Energization-Relaxation Channel Model for chloride pumping by phR.** The electrogenic steps are indicated by open arrows. The time constants and relative amplitudes are shown beside the arrows. An intermediate state between N and O has not been detected experimentally. HR′ in Váró *et al.* (*21*) was omitted for simplicity. The model is a simplified description of the chloride pump mechanism of phR and many details require further examination. See text for explanation.

We thank K. Morizumi, S. Nishino, and T. Ohtaki (Toray Industries, Inc.) for Lumirror, J.K. Lanyi (University of California, Irvine) for D96N, R. Needleman (Wayne State University) for the shR- and phR-overproducing strains and their membranes, and M. Stumpp (Tokyo Institute of Technology) for critical reading of the manuscript.

REFERENCES

1. Drachev, L.A., Jasaitis, A.A., Kaulen, A.D., Kondrashin, A.A., Liberman, E.A., Nemecek, I.B., Ostroumov, S.A., Semenov, A. Yu., and Skulachev, V.P. (1974) Direct measurement of electric current generation by cytochrome oxidase, H^+-ATPase and bacteriorhodopsin. *Nature* **249**, 321-323
2. Drachev, L.A., Frolov, V.N., Jasaitis, A.A., Kaulen, A.D., Liberman, E.A., Ostroumov, S.A., Plakunova, V.G., Semenov, A. Yu., and Skulachev, V.P. (1976) Reconstitution of biological molecular generators of electric current bacteriorhodopsin. *J. Biol. Chem.* **251**, 7059-7065
3. Drachev, L.A., Kaulen, A.D., Ostroumov, S.A., and Skulachev, V.P. (1978) Time resolution of the intermediate steps in the bacteriorhodopsin-linked electrogenesis. *FEBS Lett.* **87**, 161-167
4. Drachev, L.A., Kaulen, A.D., Semenov, A. Yu., Severina, I.I., and Skulachev, V.P. (1979) Lipid-Impregnated filters as a tool for studying the electric current-generating proteins. *Anal. Biochem.* **96**, 250-262
5. Holz, M., Lindau, M., and Heyn, M.P. (1988) Distributed kinetics of the charge movements in bacteriorhodopsin: Evidence for conformational substates. *Biophys. J.* **88**, 623-633
6. Drachev, L.A., Kaulen, A.D., Khitrina, L.V., and Skulachev, V.P. (1981) Fast stages of photoelectric processes in biological membranes. I. Bacteriorhodopsin. *Eur. J. Biochem.* **117**, 461-470
7. Holz, M., Drachev, L.A., Mogi, T., Otto, H., Kaulen, A.D., Heyn, M.P., Skulachev, V.P., and Khorana, H.G. (1989) Replacement of aspartic acid-96 by asparagine in bacteriorhodopsin slows both the decay of the M intermediate and the associated proton movement. *Proc. Natl. Acad. Sci. USA* **86**, 2167-2171
8. Otto, H., Marti, T., Holz, M., Mogi, T., Lindau, M., Khorana, H.G., and Heyn, M.P. (1989) Aspartic acid-96 is the internal proton donor in the reprotonation of the Schiff base of bacteriorhodopsin. *Proc. Natl. Acad. Sci. USA* **86**, 9228-9232

9. Gerwert, K., Hess, B., Soppa, J., and Oesterhelt, D. (1989) Role of aspartate-96 in proton translocation by bacteriorhodopsin. *Proc. Natl. Acad. Sci. USA* **86**, 4943-4947
10. Otto, H., Marti, T., Holz, M., Mogi, T., Stern, L.J., Engel, F., Khorana, H.G., and Heyn, M.P. (1990) Substitution of amino acids Asp-85, Asp-212, and Arg-82 in bacteriorhodopsin affects the proton release phase of the pump and the pK of the Schiff base. *Proc. Natl. Acad. Sci. USA* **87**, 1018-1022
11. Dickopf, S., Alexiev, U., Krebs, M.P., Otto, H., Mollaaghhaababa, R., Khorana, H.G., and Heyn, M.P. (1995) Proton transport by a bacteriorhodopsin mutant, aspartic acid-85→asparagine, initiated in the unprotonated Schiff base state. *Proc. Natl. Acad. Sci. USA* **92**, 11519-11523
12. Kimura, Y., Vassylyev, D.G., Miyazawa, A., Kidera, A., Matsushima, M., Mitsuoka, K., Murata, K., Hirai, T., and Fujiyoshi, Y. (1997) Surface of bacteriorhodopsin revealed by high-resolution electron crystallography. *Nature* **389**, 206-211
13. Luecke, H., Richter, H.-T., and Lanyi, J.K. (1998) Proton transfer pathways in bacteriorhodopsin at 2.3 angstrom resolution. *Science* **280**, 1934-1937
14. Lanyi, J.K. (1990) Halorhodopsin, a light-driven electrogenic chloride-transport system. *Physiol. Rev.* **70**, 319-330
15. Oesterhelt, D. (1995) Structure and function of halorhodopsin. *Isr. J. Chem.* **35**, 475-494
16. Bamberg, E., Hegemann, P., and Oesterhelt, D. (1984) Reconstitution of the light-driven electrogenic ion pump halorhodopsin in black lipid membranes. *Biochim. Biophys. Acta* **773**, 53-60
17. Dèr, A., Fendler, K., Keszthelyi, L., and Bamberg, E. (1985) Primary charge separation in halorhodopsin. *FEBS Lett.* **187**, 233-236
18. Bamberg, E., Tittor, J., and Oesterhelt, D. (1993) Light-driven proton or chloride pumping by halorhodopsin. *Proc. Natl. Acad. Sci. USA* **90**, 639-643
19. Kalaidzidis, I.V., Kalaidzidis, Y.L., and Kaulen, A.D. (1998) Flash-induced voltage changes in halorhodopsin from *Natronobacterium pharaonis*. *FEBS Lett.* **427**, 59-63
20. Várő, G., Zimányi, L., Fan, X., Sun, L., Needleman, R., and Lanyi, J.K. (1995) Photocycle of halorhodopsin from *Halobacterium salinarium*. *Biophys. J.* **68**, 2062-2072
21. Várő, G., Brown, L.S., Sasaki, J., Kandori, H., Maeda, A., Needleman, R., and Lanyi, J.K. (1995) Light-driven chloride ion transport by halorhodopsin from *Natronobacterium pharaonis*. 1. The photochemical cycle. *Biochemistry* **34**, 14490-14499
22. Várő, G., Needleman, R., and Lanyi, J.K. (1995) Light-driven chloride ion transport by halorhodopsin from *Natronobacterium pharaonis*. 2. Chloride release and uptake, protein conformation change, and thermodynamics. *Biochemistry* **34**, 14500-14507
23. Muneyuki, E., Okuno, D., Yoshida, M., Ikai, A., and Arakawa, H. (1998) A new system for the measurement of electrogenicity produced by ion pumps using a thin polymer film: Examination of wild type bR and the D96N mutant over a wide pH range. *FEBS Lett.* **427**, 109-114
24. Muneyuki, E., Ikematsu, M., and Yoshida, M. (1996) $\Delta\mu_H$-dependency of proton translocation by bacteriorhodopsin and a stochastic energization-relaxation channel model. *J. Phys. Chem.* **100**, 19687-19691
25. Oesterhelt, D. and Stoeckenius, W. (1974) Isolation of the cell membrane of *Halobacterium halobium* and its fractionation into red and purple membrane. *Methods Enzymol.* **31**, 667-678
26. Ohtani, H., Naramoto, S., and Yamamoto, N. (1994) Laser photolysis of the purple membrane of *Halobacterium halobium* in the photostationary state: the photobranching process from O640 intermediate. *Photochem. Photobiol.* **60**, 394-398
27. Rüdiger, M. and Oesterhelt, D. (1997) Specific arginine and threonine residues control anion binding and transport in the light-driven chloride pump halorhodopsin. *EMBO J.* **16**, 3813-3821
28. Nagel, G., Kelety, B., Möckel, B., Büldt, G., and Bamberg, E. (1998) Voltage dependence of proton pumping by bacteriorhodopsin is regulated by the voltage-sensitive ratio of M1 to M2. *Biophys. J.* **74**, 403-412
29. Ames, J.B., Raap, J., Lugtenburg, J., and Mathies, R.A. (1992) Resonance Raman study of halorhodopsin photocycle kinetics, chromophore structure, and chloride-pumping mechanism. *Biochemistry* **31**, 12546-12554
30. Walter, T.J. and Braiman, M.S. (1994) Anion-protein interactions during halorhodopsin pumping: halide binding at the protonated Schiff base. *Biochemistry* **33**, 1724-1733
31. Schobert, B. and Lanyi, J.K. (1986) Electrostatic interaction between anions bound to site I and the retinal Schiff base of halorhodopsin. *Biochemistry* **25**, 4163-4167
32. Pande, C., Lanyi, J.K., and Callender, R.H. (1989) Effects of various anions on the Raman spectrum of halorhodopsin. *Biophys. J.* **55**, 425-431
33. Braiman, M.S., Walter, T.J., and Briercheck, D.M. (1994) Infrared spectroscopic detection of light-induced change in chloride arginine interaction in halorhodopsin. *Biochemistry* **33**, 1629-1635